Mapping of the Osteochondral Defect

11

Shanmugasundaram Saseendar,
Saseendar Samundeeswari,
Anandapadmanabhan Jayajothi,
and Asode Ananthram Shetty

It was eerie. I saw myself in that machine.
I never thought my work would come to this.
Isidor Isaac Rabi
(American physicist, won Nobel Prize in Physics (1944) for discovery of nuclear magnetic resonance)

11.1 Introduction

Articular cartilage has limited capacity for spontaneous repair and hence demand an early and accurate diagnosis and intervention. This chapter intends to summarize the various magnetic resonance imaging (MRI) techniques to identify and quantify articular cartilage injury in an orthopedic surgeon's perspective.

S. Shanmugasundaram (✉)
Specialist Knee and Shoulder Surgery and Cartilage Reconstruction, Department of Orthopaedics, Apollo Hospital, Muscat, Sultanate of Oman

S. Saseendar
Orthopaedic Surgeon, CARE Sports Injury Clinic, Puducherry, India

A. Jayajothi
Consultant Radiologist, Department of Radiodiagnosis, Swansea Bay University Health Board NHS, Port Talbot, UK

A. A. Shetty
Consultant Orthopaedic Surgeon, Faculty of Health and Social Sciences, Chatham Maritime, Canterbury Christ Church University, Kent, UK

11.2 Basics of Magnetic Resonance Imaging

Magnetic resonance (MR) imaging is the most important imaging modality for the evaluation of traumatic or degenerative cartilaginous lesions in the knee [1]. Currently, standardized cartilage-sensitive pulse sequences are available for all joints.

Volumetric (quantitative) MR imaging is likely to become more available to standardized work stations, permitting the longitudinal assessment of cartilage volume over time.

One of the major advantages of MRI is that it allows the manipulation of contrast to highlight different tissue types and also provides multiplanar capability with spatial resolution that approaches that of computed tomography (CT), without the potentially harmful ionizing radiations of radiographs and CT [2].

It is essential to understand the basic principles of the functioning of MRI to understand how cartilage mapping functions.

A. Gobbi et al. (eds.), *Joint Function Preservation*, https://doi.org/10.1007/978-3-030-82958-2_11

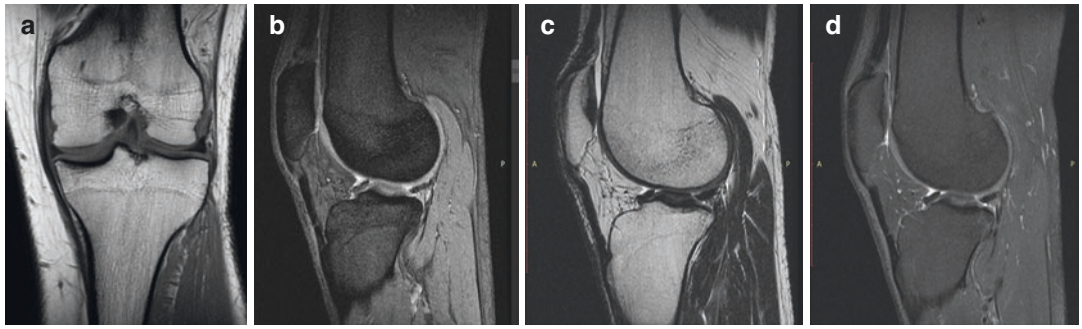

Fig. 11.1 (**a**) Coronal T1, (**b**) Sagittal GRE, (**c**) Sagittal T2, and (**d**) Sagittal PD fat-saturated images of knee joint

MRI scanners can be grouped roughly based on field strength into ultralow-field scanners (<0.1 Tesla (T)), low-field scanners (0.3 to 0.7 T), and high-field scanners (>1.0 T).

Low-field systems have shown poorer diagnostic performance in comparison to high-field systems, especially when assessing partial-thickness cartilage damage [3].

High-field scanners generate higher signal-to-noise images and allow shorter scanning times, thinner scan slices, and smaller fields of view, the most commonly used scanner being the 1.5 T MRI.

(a) **Surface coils** are devices that act as antennae placed close to the joint or limb and markedly improve signal and resolution and help achieve good image quality and visualization of cartilage. Surface coils for wrist, shoulder, knee, and ankle are currently standard.

(b) **How an MRI scan is performed:** The patient is placed in a strong magnetic field many times stronger than the earth's magnetic field. The magnetic force affects the nuclei of elements with odd numbers of protons or neutrons within the field, the most abundant being hydrogen, which is plentiful in water and fat. These hydrogen nuclei, which are essentially protons, align themselves with respect to the strong magnetic field. In this steady state, a radiofrequency (RF) pulse excites the magnetized protons and perturbs the steady state. A receiver coil listens for an emitted RF signal that is generated as these excited protons relax or return to equilibrium. This emitted signal is used to create the MR image.

Musculoskeletal MRI examinations primarily use spin-echo (SE) technique (Fig. 11.1), which produces T1-weighted, proton density (PD), and T2-weighted images. T1 and T2 are tissue-specific characteristics. These values reflect measurements of the rate of relaxation to the steady state. By varying the timing of the application of RF pulses (TR, or repetition time) and the timing of acquisition of the returning signal (TE, or echo time), an imaging sequence can accentuate T1 or T2 tissue characteristics. In most cases, fat has a high signal (bright) on T1-weighted images and fluid has a high signal on T2-weighted images. Structures with little water or fat, such as cortical bone, tendons, and ligaments, are hypointense (dark) in all types of sequences.

Improvements in MR techniques led to the development of a relatively new techniques called the fast spin-echo (FSE) that allows faster imaging, thereby improving patient tolerance and decreasing motion artifacts. Fat signal in FSE images remains fairly intense, requiring fat-suppression techniques, e.g., chemical-shift fat-suppression and short tau inversion recovery (STIR) sequence. These fat-suppression techniques help in the detection of edema in both bone marrow and soft tissue and hence are named "fluid-sensitive" sequences (Fig. 11.2). Another fast imaging method, gradient-echo technique, can be used selectively for cartilage imaging (such as for the glenoid labrum).

Fig. 11.2 Coronal section of knee: STIR image showing marrow edema (arrow) in the medial tibial condyle

The general consensus is IM-weighted sequences have echo times (TE) in the range of 30–60 ms and T2-weighted sequences have TE of 70–80 ms and PD-weighted sequences have TE of 10–30 ms [3]. In general, fat-suppressed, fluid-sensitive IM-weighted FSE sequences have been the most useful standard imaging for cartilage. With IM- and T2-weighted FSE sequences, normal hyaline cartilage is intermediate in signal and fluid is bright, allowing good contrast to identify surface abnormalities as well as pathologies of the cartilage matrix. However, they cannot characterize the severity of cartilage degeneration as validated by histology [4].

Diagnostic performance for cartilage lesions increases when different imaging planes are used in comparison to a single imaging plane alone. Isometric/volume acquisition also reduces time duration and the ability to multiplanar reconstruction of images, thereby reducing the time taken as well as reducing the risk of motion artifacts (Fig. 11.3).

(c) **MRI sequences in cartilage mapping:** MR imaging techniques can be divided into two broad categories based on their usefulness for a) morphologic and b) compositional evaluation. **Morphologic assessment techniques** provide accurate information on the structure of the cartilage and identify fissuring, focal or diffuse, partial- or full-thickness cartilage loss and hence are used for semiquantitative or quantitative assessment of the cartilage. They include conventional SE, GRE, FSE, and more advanced isotropic three-dimensional (3D) SE and GRE sequences. Objective evaluation scores have been proposed to describe focal cartilage defects in the knee, the most commonly used being the Outerbridge score. The score was primarily developed for arthroscopic assessment of the cartilage, but has been modified and extended for use with MRI [5].

Modified Outerbridge grading of cartilage:

- **Grade I:** Focal areas of hyperintensity with normal contour.
- **Grade II:** Swelling/ fraying of articular cartilage extending to surface.
- **Grade III:** Partial-thickness cartilage loss with focal ulceration.
- **Grade IV:** Full-thickness cartilage loss with underlying bone reactive changes.

On the other hand, **compositional assessment techniques** identify changes in the composition of the cartilage with special address to the water content and proteoglycan and collagen content. These techniques include T2 mapping, delayed gadolinium-enhanced MR imaging of cartilage (dGEMRIC), T1rho imaging, sodium imaging, and diffusion-weighted imaging.

11.3 Morphologic Assessment of Cartilage

(a) **Two-dimensional SE and Fast SE Imaging**: 2D or multisection T1-weighted, PD-weighted, and T2-weighted imaging sequences with or without fat-suppression are the most commonly used imaging sequences for the assessment of joint cartilage (Fig. 11.1). **T1-weighted images** show intrasubstance anatomic detail of hyaline cartilage but do not provide good contrast

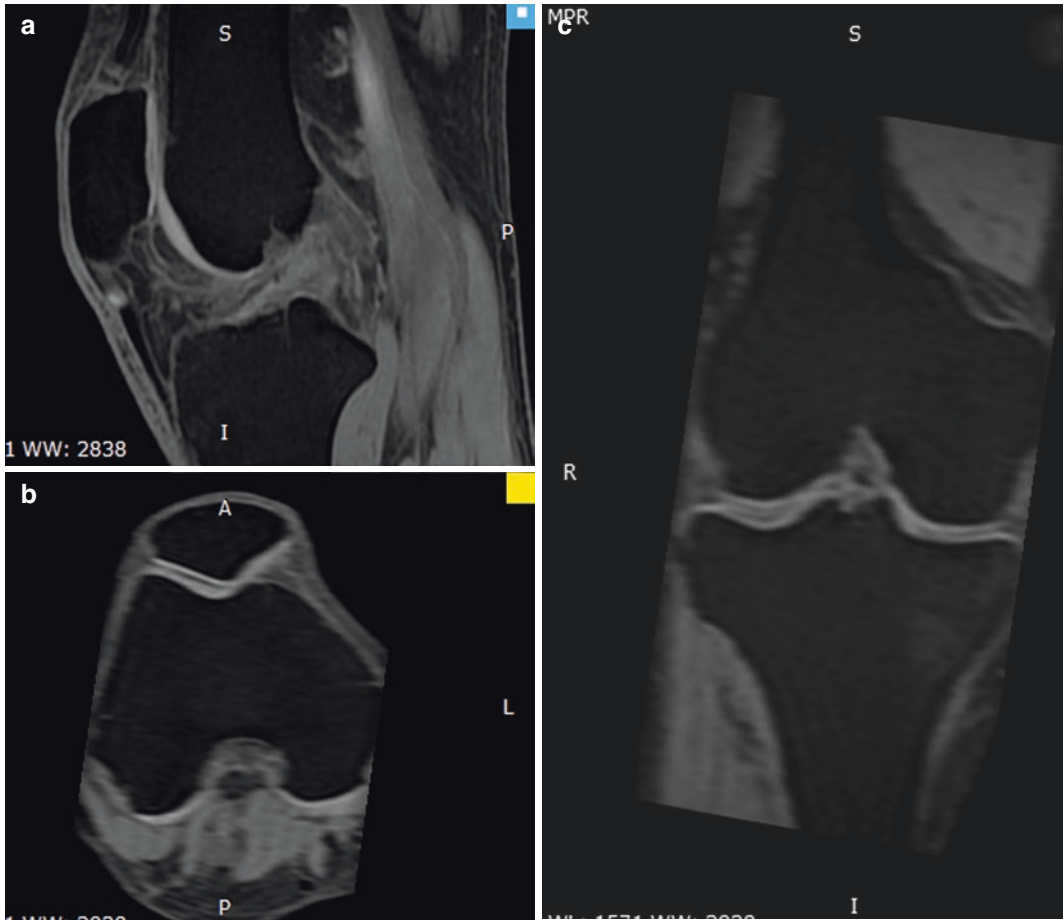

Fig. 11.3 Multiplanar image reconstruction using single isometric volume acquisition: (**a**) sagittal, (**b**) axial, (**c**) coronal

between joint fluid and the cartilage and also carry poor capability for depicting ligament injuries and may lead to overestimation of meniscal abnormalities. **T2-weighted imaging** provides good contrast between the cartilage surface and joint effusion, which is useful for detecting focal areas of delamination or other defects, whereas internal cartilage signals are weakened. **Proton density-weighted imaging** is mostly the main workhorse in MSK imaging, carrying the benefit of both depicting surface cartilaginous defects as well as abnormalities of internal cartilage composition. **Intermediate-weighted sequences** are being used more commonly in recent times. They provide the combination of the contrast advantage of proton density weighting and also a higher signal intensity in cartilage than standard T2-weighted sequences, allowing better differentiation between cartilage and subchondral bone.

(b) **Two-dimensional fast or turbo SE imaging** sequences are techniques where multiple echoes are acquired with each sequence repetition. Hence, acquisition time is shorter than that with standard SE sequences and signal-to-noise (SNR) and contrast-to-noise (CNR) are higher. It is the technique most often used in clinical practice for the assessment of knee joint abnormalities, including cartilaginous lesions.

(c) **Proton density-weighted** and **T2-weighted FSE imaging techniques** are well suited for

morphologic assessments of articular cartilage as well as menisci and ligamentous structures, providing information of a quality comparable to that obtained in surgery [6]. Although fast SE sequences provide excellent SNR and contrast between tissues of interest, 2D fast SE imaging may suffer from anisotropic voxels, section gaps, and partial volume effects. Furthermore, this technique requires the acquisition of image data in multiple planes.

(d) **MR Arthrography**: Direct MR arthrography with use of T1-weighted pulse sequences (Fig. 11.4)[7] following intra-articular injection of gadolinium chelates has been shown to represent a reliable imaging technique for the detection of surface lesions of articular cartilage with high sensitivity and specificity [8]. The injected fluid produces high contrast between joint space, cartilage, and subchondral bone, and at the same time distends the joint and thus, improves the separation of corresponding joint surfaces, such as the chondral surfaces of the femur and the acetabulum at the hip joint. However, this technique is of limited use for osteoarthritis imaging due to its invasive nature.

Fig. 11.4 Direct MR arthrography of the knee joint, T1-weighted SE showing hyperintense synovial fluid. There is a cartilage defect within the patella representative of first-stage chondromalacia (Reproduced with permission from Imhof et al. [7])

(e) **Three-dimensional MR Imaging**: These sequences generate isotropic voxels and allow high-quality reformations in any plane. Thus, it may be possible to only obtain one high spatial-resolution image dataset and get the additional planes as reformations. This would potentially save acquisition time and shorten patient examinations substantially. These techniques are considered the standard technique for morphologic evaluations of knee cartilage because they offer higher sensitivity than 2D techniques and provide excellent depiction of cartilaginous defects, comparable to that achieved with arthroscopy [9]. The commonly used 3D imaging sequences include 3D FSE, 3D GRE, 3D SPGR. The terminologies of these sequences could vary depending on the manufacturer, though the technique and imaging parameters remain the same.

(f) **Limitations:**

1. Small focal lesions and fissures are obscured because of the lack of reliable contrast between cartilage and fluid.
2. The gradient-echo sequences are not suited to visualize bone marrow pathology and are very limited in assessing menisci, ligaments, and tendons and are best suited only for quantitative measurement of volume and thickness of cartilage [10],
3. They overestimate cartilage, ligament, and meniscal tear.
4. Long acquisition times may lead to motion artifacts and less accurate measurements although these problems may be less severe with current MR imaging systems.
5. Fourth, the technique is highly vulnerable to susceptibility artifacts. In a recent study, high-resolution images of knee joint cartilage were obtained with an increased SNR, better cartilage-to-fluid contrast, and shorter acquisition time

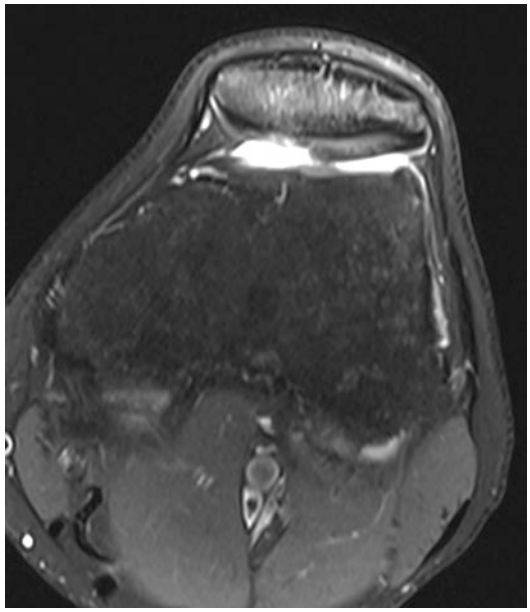

Fig. 11.5 Axial fat-suppressed 3D DESS sequence depicting a partial-thickness cartilage defect in the interfacetal patellar cartilage (Courtesy: Dr. Ananthram Shetty, Spire Alexandra Hospital, UK, Dr. Stelzeneder, Medical University of Vienna, Austria)

with combined IDEAL and SPGR sequences than with a standard fat-saturated SPGR sequence alone [11].

Other 3D sequences have been described as modifications and improvements over these sequencing techniques for better visualization of the cartilage and improving the SNR and CNR, e.g., fast low-angle shot (FLASH) imaging, 3D-driven equilibrium Fourier transform (DEFT), balanced steady-state free precision (bSSFP), and 3D dual-echo steady-state (DESS) imaging (Fig. 11.5).

11.4 Compositional Assessment of the Cartilage Matrix

In addition to assessing cartilage pathology as well as thickness and volume, recent studies have shown the potential of MRI parameters to reflect changes in biochemical composition of cartilage with early OA.

These techniques include T2 quantification, T1rho quantification, and delayed Gadolinium-enhanced MRI of cartilage (dGEMRIC) [12]. These techniques allow characterization of the cartilage matrix and, potentially, quality before morphological damage occurs.

(a) **T2 Quantification:** This technique is based on the finding that increasing T2 relaxation time is proportional to the distribution of cartilage water and is sensitive to small water content changes [13] and is inversely proportional to the distribution of proteoglycans. Thus, measurement of the spatial distribution of the T2 reflecting areas of increased and decreased water content may be used to quantify cartilage degeneration before morphologic changes are appreciated (Figs. 11.6 and 11.7). Aging is associated with an asymptomatic diffuse increase in T2 of the transitional zone of articular cartilage in the senescent cartilage which is different from the focal increased T2 observed in damaged articular cartilage [14].

(b) **T1rho Quantification:** A different parameter that has been proposed to measure cartilage composition is 3D T1rho relaxation mapping (Fig. 11.8) [13, 15]. Loss of glycosaminoglycans (GAG) is reflected in measurements of T1rho due to less-restricted motion of water protons.

Both T2- and T1rho-measurements carry the benefit of identifying biochemical changes before the actual development of cartilage degeneration in asymptomatic subjects [16] and also being noninvasive and not requiring contrast injection.

(c) **Delayed Gadolinium-enhanced MRI of Cartilage (dGEMRIC):** Cartilage consists of approximately 70% water and the remainder predominantly of type II collagen fibers and GAG. These GAG macromolecules contain negative charges that attract sodium ions (Na+). One of the most commonly used MRI

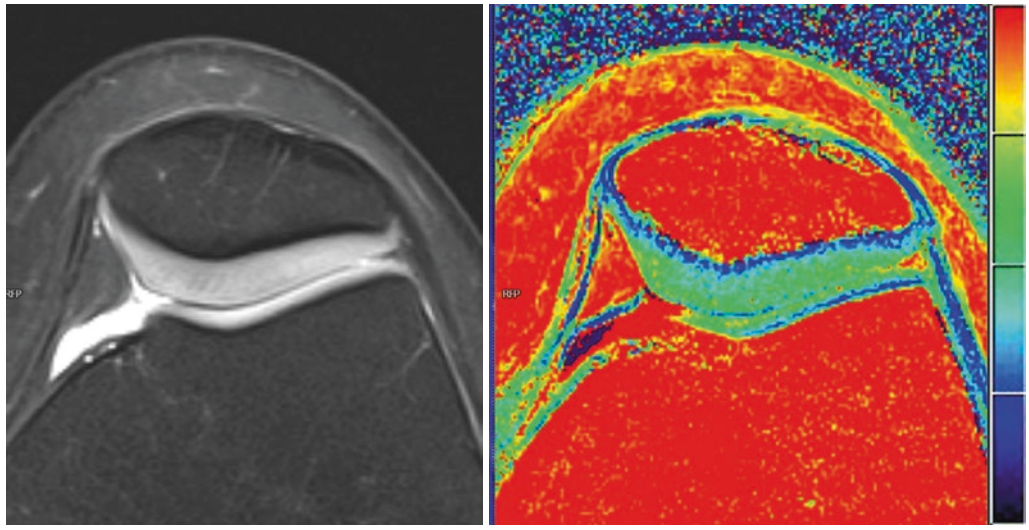

Fig. 11.6 Standard T2 and corresponding T2 mapping shows a normal appearance of the patellar and femoral trochlear articular cartilage. The deep layer of the cartilage appears blue and the superficial layer appears green on T2 mapping images. (Courtesy: Dr. Alvaro Zamorano, Dr. Jorge Diaz, University of Chile Clinical Hospital, Chile)

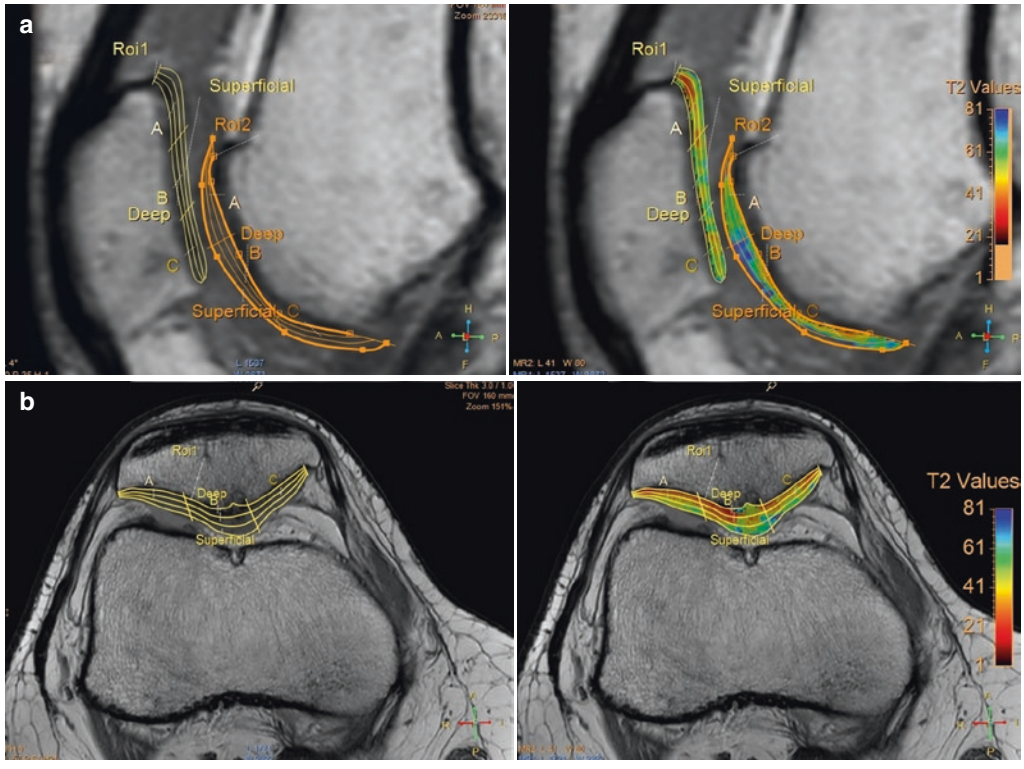

Fig. 11.7 Sagittal (**a**) and axial (**b**) MRI image of the knee showing the patellar and femoral articular cartilage T2 mapping showing red to orange marking in deeper layer of cartilage (lower T2 relaxation) and the green marking in superficial layer of cartilage (higher T2 relaxation). Zone B of both patellar and femoral articular cartilage show blue regions (higher abnormal T2 relaxation) indicating early cartilage damage (Courtesy: Dr. Raju Vaishya, Dr. Nitin Ghonge, Indraprastha Apollo Hospitals, India)

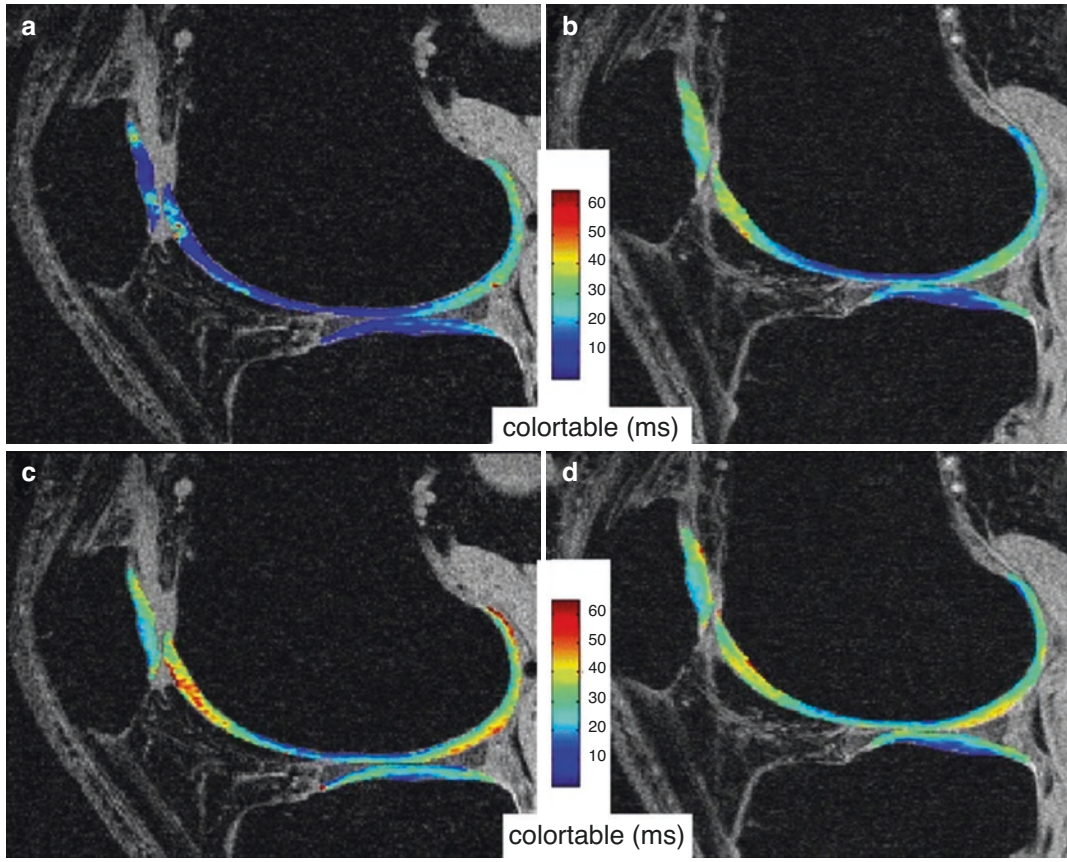

Fig. 11.8 Color-coded T2 (**a**, **b**) and T1rho (**c**, **d**) maps overlaid on a sagittal SPGR image in a 35-year-old male before (**a, c**) and after (**b, d**) a marathon. After the marathon (**b**), T2 times were significantly increased, mainly in the patella and the trochlea, indicating cartilage edema with increased water content secondary to the physical stress. The patella, femur, and lateral tibia plateau showed only a small increase in T1rho times after the marathon (**d**), indicating only a subtle change in cartilage macromolecular matrix (Reproduced without changes from Link et al. [15] (Licensed under CC by 4.0)

contrast agents Gd-DTPA2 has a negative charge and will therefore not penetrate cartilage in areas of high GAG concentrations. It gets distributed in higher concentrations in areas with lower GAG concentration and thus pathologic cartilage composition. Concentrations of Gd-DTPA2 in cartilage can be measured, reflecting the composition of cartilage (Fig. 11.9) [17, 18]. dGEMRIC measurements of GAG have correlated well with concentrations measured with biochemistry and histology [12, 19].

11.5 Clinical Cartilage Imaging

(a) **Cartilage Imaging in Traumatic Lesions**: Articular cartilage lesions are common after injury especially in the knee. MRI serves as a noninvasive option for the evaluation of the cartilage and other structures of the joint. Early identification of such lesions and cartilage repair when indicated may offer the possibility for patients to avoid the development of osteoarthritis or delay its progression. Newly developed cartilage repair techniques,

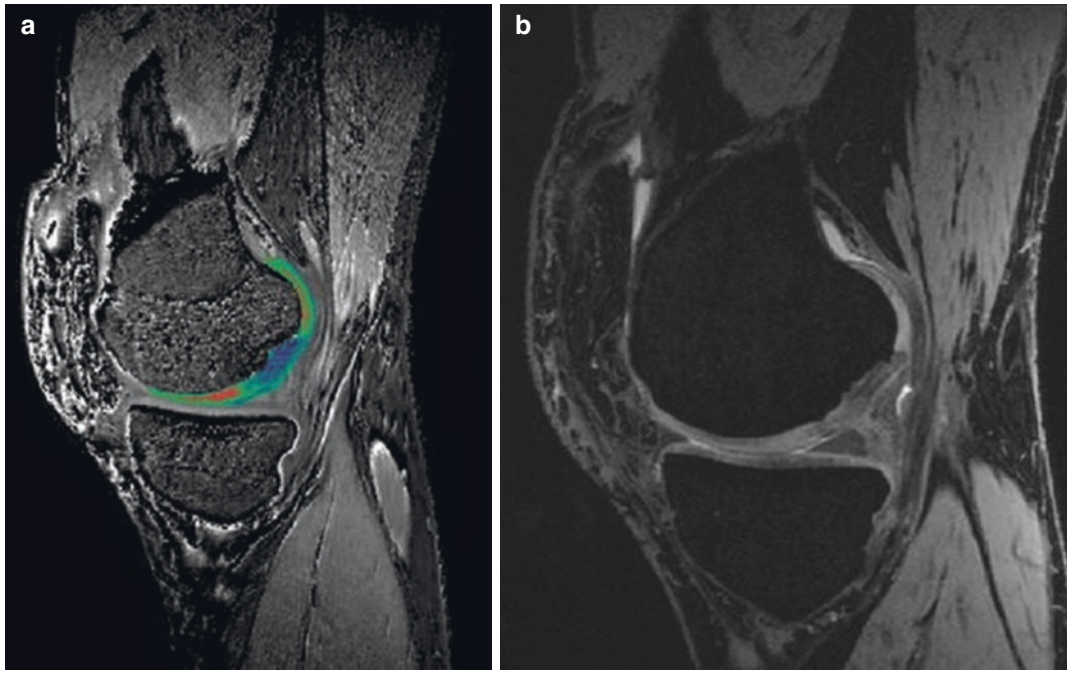

Fig. 11.9 A dGEMRIC image of a matrix-associated ACT 2 years after surgery. (**a**) The cartilage layer of the graft shows different T1 values, representing proteoglycan concentration, compared with hyaline cartilage. (**b**) a 3D-GRE image of the same patient, which shows morphology of cartilage implant with hypointense signal alteration of the cartilage implant in comparison with normal hyaline cartilage (Reproduced without changes from Trattnig et al. [17] (Licensed under CC by 4.0)

including marrow-stimulation techniques, osteochondral grafting, autologous chondrocyte implantation and require high-quality follow-up to assess healing [20].

Adequate preoperative imaging is required to study the lesions carefully. It is important to differentiate between an isolated cartilage injury from an osteochondral fracture as the treatment options and protocol for rehabilitation would vary tremendously. Osteochondral injuries can be recognized by the presence of hyperintense fatty marrow attached to the cartilage fragment or by the absence of the thin, low-signal-intensity subchondral plate between the cartilage and the bone (Fig. 11.10).

(b) **Cartilage Imaging in Osteoarthritis**: Lot of recent research has gone into MR imaging of osteoarthritis. Various noninvasive and invasive regenerative options have been proposed for the treatment of osteoarthritis. Establishing their efficacy would need objective morphological and compositional assessment of the cartilage, in order to assess both the extent of structural cartilage healing and the quality of the regenerate.

MRI, especially T2 mapping, can identify both early osteoarthritis changes characterized by cartilage softening and later by cartilage thinning, and also more severe changes such as subchondral sclerosis, cyst, and osteophyte formation. Both quantitative and qualitative assessment of such lesions is possible. Figure 11.11 depicts T2 mapping of an adult patient with significant medial knee osteoarthritis.

(c) **Cartilage Imaging in Repair**: Hyaline cartilage is an avascular and aneural structure that carries little to no inherent capacity for spontaneous repair [21]. The field of cartilage repair has been rapidly expanding in an attempt to bring about healing of the defect

Fig. 11.10 (**a**) Sagittal T1, (**b**) Coronal T1, (**c**) PD fat-saturated, (**d**) STIR images of the ankle joint demonstrating osteochondral lesion of the talus with an undisplaced fragment and high signal rim around the osteochondral defect typical for a grade III lesion

created by chondral and osteochondral damage. The techniques include simple debridement, abrasion chondroplasty and microfracture, autologous osteochondral transplantation, allograft transplantation, and autologous chondrocyte implantation. The basic biological principles of these methods vary tremendously. Confirming improvement in the structure and composition of the new cartilage tissue would need dedicated MR imaging techniques.

Various scoring systems exist to objectively evaluate the repair tissue. The MOCART classification is the most frequently scoring system based on MRI for postoperative cartilage repair tissue evaluation [22, 23]. It is a 9-part and 29-item scoring system, resulting in a repair tissue score between 0 and 100 points where 100 points indicates the best imaginable score and 0 points indicates the worst imaginable score.

1. **Microfracture**: Microfracture is one of the most popular resurfacing techniques. It consists of debriding calcified cartilage and drilling small holes into the subchondral bone. The principle behind this technique is to allow release of multipotential stem cells from the marrow that would encourage healing of the defect with reparative fibrocartilage. The out-

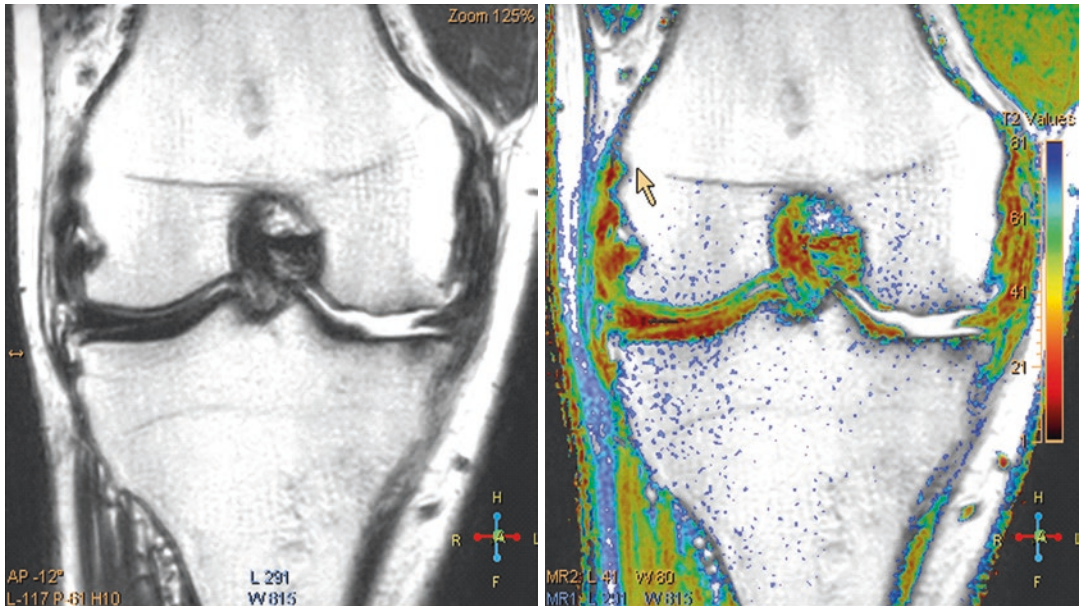

Fig. 11.11 T2 mapping of the knee joint demonstrating degenerative changes with cartilage thinning, subchondral sclerosis, and near-complete loss of medial tibial and femoral articular cartilage with rarefaction (Courtesy: Dr. Manuel Mosquera, Clinica la Carolina, Dr. Ruben Guzman, Clinica el Rosario, Colombia)

comes of this technique have been shown to be dependent on good MRI fill grade in addition to low body mass index (BMI) and short duration of preoperative symptoms [24].

The response to microfracture is characterized by initial hyperintensity due to increased mobility of water in the newly formed matrix [24, 25] in addition to underlying bone marrow edema that decreases progressively. Overgrowth of subchondral bone has also been reported following microfracture along with corresponding thinning of the overlying repair tissue [24, 25].

The significance of subchondral bone overgrowth is not yet certain, but could result from excessive removal of subchondral bone, leading to overstimulation for endochondral ossification [26]. Preservation of the subchondral bone has been emphasized recently in the conceptualization of nanofracture technique. MRI can also help in assessing peripheral integration of the repair tissue. T2 mapping can help in assessing the quality of cartilage repair. T2 mapping following microfracture has usually produced prolonged T2 relaxation times in comparison to the adjacent and opposite hyaline cartilage (Fig. 11.12) [24].

2. **Osteochondral Autografts and Allografts**: Osteochondral autograft or allograft transplantation consists of harvesting one or more plugs from a less important part of a joint, most commonly the intercondylar notch region, and transferring into the defect in a weight-bearing portion of the joint. Bone-cartilage plug allografts are usually reserved for large defects while autografts are the choice for smaller defects.

In addition to patient reported outcome measures, objective evaluation of repair provides insight into the healing capacity of the technique and possibly the long-term outcomes of the treatment. MRI assessment has largely replaced histologic evaluation of biopsy specimens as the method for objective assessment (Fig. 11.13) [17].

Brown et al. [25] proposed parameters to be assessed in an MR imaging after cartilage transplantation or microfracture: signal intensity of the repair cartilage, presence of delamination, interface with the native cartilage,

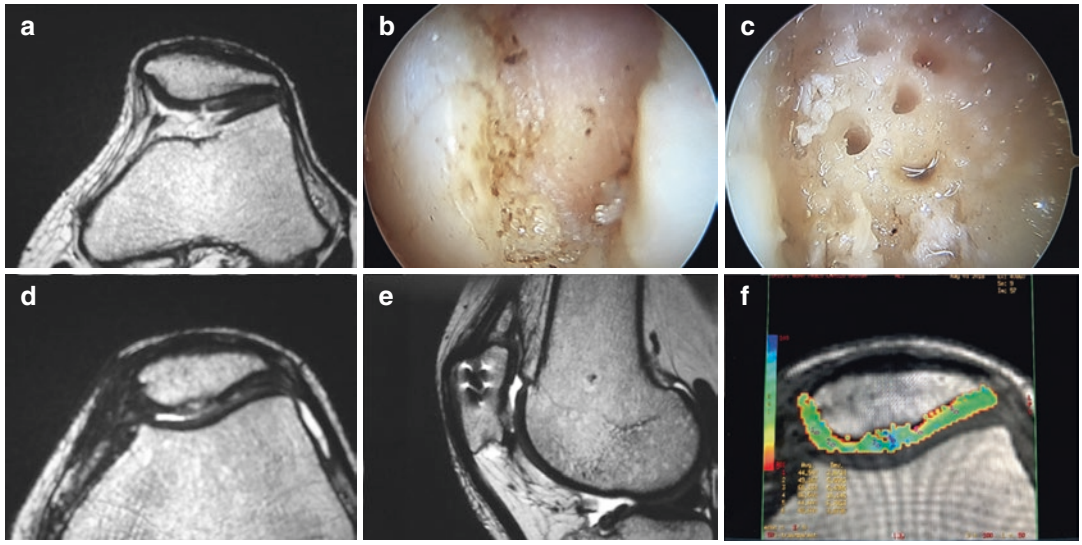

Fig. 11.12 (**a**) Preoperative MRI axial section T2-weighted image of the patellofemoral joint following patella dislocation, showing a linear fissure and delamination in the ridge and lateral facet of patella; arthroscopic image of cartilage defect in the patella before (**b**) and after (**c**) microfracture; postoperative sagittal T2-weighted (**d**), axial (**e**), and T2 mapping (**f**) images demonstrating repair tissue with slightly higher relaxation values (Courtesy: Dr. David Figueroa, Clinica Alemana, Chile)

Fig. 11.13 Normal cartilage integration of osteochondral autografts in the weight bearing region of the femoral condyle in a patient 2 years after osteochondral autografts (Reproduced without changes from Trattnig et al. [17] (Licensed under CC by 4.0)

percentage fill of the lesion in coronal and sagittal images, integrity of the articular cartilage in the surrounding environment, including cartilage in the adjacent and opposite surfaces.

Cartilage-sensitive MR imaging and T2 mapping in a canine model showed trabecular osseous integration in 89% of specimens at 6 months. However, on histology, the cartilage showed incomplete or no integration between the host and graft surfaces in both autografts and allografts, asserting that articular cartilage does not regenerate completely across gaps [27]. MRI can also assess the degree of offset of the subchondral plate in relation to the host tissue. Thus, MRI can provide more detailed information than the invasive second-look arthroscopy. T2 relaxation times observed after autologous osteochondral transplantation have been found to be closer to that of the host tissue. MRI can also help in assessing the surface alignment of the graft plug in relation to the rest of the joint surface. Proud plugs are associated with increased contact pressures and formation of subchondral cavitations suggesting excessive motion between the graft and recipient site.

While cartilage-sensitive sequences assess the integrity of the cartilage and its surface, fat-suppressed images help assess the relation of the graft and the host at the subchondral bone. Low signal intensity on all pulse sequences strongly suggests loss of bone viability, which may lead to eventual implant failure. However, care must be taken to avoid mistaking the low-signal-intensity of trabecular compression in a "press fit" fixation for failure of the graft to incorporate. If instrumentation had been used, modification of pulse sequence would be necessary to reduce susceptibility artifacts in the presence of metallic fixation.

3. **Autologous Chondrocyte Implantation**: Autologous chondrocyte implantation is an example of tissue engineering technique for cartilage reconstruction. It consists of three key elements—a matrix scaffold, cells and signaling molecules, including growth factors or genes [21]. An MRI done after ACI would need to assess the following parameters: fill, maturation of tissue, integration with the subchondral bone and integration with adjacent hyaline cartilage. The fill after ACI is consistently better that after microfracture (Fig. 11.14). However, graft hypertrophy is a common complication after ACI and can lead to morbidity. Hypertrophy usually occurs within the first 6 months postoperatively [25].

   In the initial few months, the repair cartilage is hyperintense due to the immature matrix and increased mobility of water. This is topped by the low-intensity periosteum [25]. The repair cartilage stays hyperintense until 8 weeks following which there is a transitional phase with lower, more inhomogeneous signal intensity for 3 to 6 months. In the final remodeling phase, the signal approaches that of the host hyaline cartilage [28].

   A good integration of the repair tissue with the underlying subchondral bone should lack fluid signals at the deep interface. The presence of persistent fluid signal intensity at this interface suggests impending delamination [29]. Peripheral integration, one of the most important factors in evaluating cartilage repair, can be evaluated with the help of high-resolution fluid-sensitive pulse sequences [20]. Edge integration is known to take up to 2 years and is seen as a lack of fluid intensity between the native and repair cartilage [28]. Finally, dGEMRIC techniques can be used to evaluate the quality of the repair tissue. The glycosaminoglycan levels have been found to reach levels comparable to the adjacent host hyaline cartilage after 12 months.

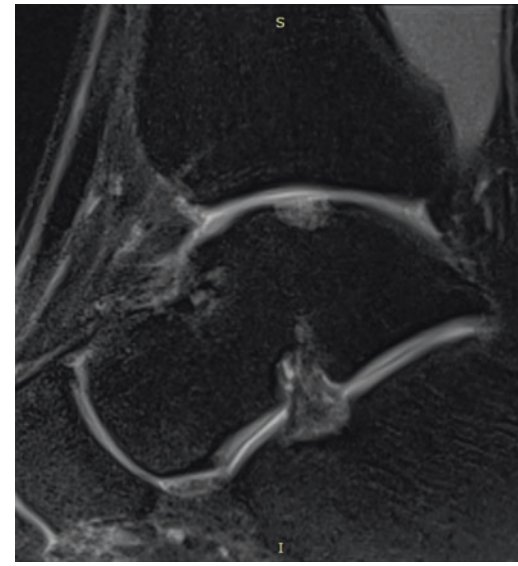

Fig. 11.14 Postoperative sagittal STIR MRI sequence of Fig. 11.10 following autologous chondrocyte implantation, showing good repair tissue

References

1. Crema MD, Roemer FW, Marra MD, Burstein D, Gold GE, Eckstein F, Baum T, Mosher TJ, Carrino JA, Guermazi A. Articular cartilage in the knee: current MR imaging techniques and applications in clinical practice and research. Radiographics. 2011;31(1):37–61.
2. Canale ST, Beaty JH. Campbell's operative orthopaedics e-book. Philadelphia, PA: Elsevier Health Sciences; 2012.
3. Link TM. MRI of cartilage: standard techniques. In: Link TM, editor. Cartilage imaging: significance, techniques, and new developments. New York: Springer Science & Business Media; 2011.

4. Saadat E, Jobke B, Chu B, Lu Y, Cheng J, Li X, Ries MD, Majumdar S, Link TM. Diagnostic performance of in vivo 3-T MRI for articular cartilage abnormalities in human osteoarthritic knees using histology as standard of reference. Eur Radiol. 2008;18(10):2292–302.
5. Cole BJ, Malek MM. Articular cartilage lesions: a practical guide to assessment and treatment. New York: Springer Science & Business Media; 2013.
6. Kijowski R, Davis KW, Woods MA, Lindstrom MJ, De Smet AA, Gold GE, Busse RF. Knee joint: comprehensive assessment with 3D isotropic resolution fast spin-echo MR imaging—diagnostic performance compared with that of conventional MR imaging at 3.0 T. Radiology. 2009;252(2):486–95.
7. Imhof H, Nöbauer-Huhmann I, Krestan C, et al. MRI of the cartilage. Eur Radiol. 2002;12:2781–93.
8. Gagliardi JA, Chung EM, Chandnani VP, Kesling KL, Christensen KP, Null RN, Radvany MG, Hansen MF. Detection and staging of chondromalacia patellae: relative efficacies of conventional MR imaging, MR arthrography, and CT arthrography. AJR. Am J Roentgenol. 1994;163(3):629–36.
9. Disler DG, McCauley TR, Kelman CG, Fuchs MD, Ratner LM, Wirth CR, Hospodar PP. Fat-suppressed three-dimensional spoiled gradient-echo MR imaging of hyaline cartilage defects in the knee: comparison with standard MR imaging and arthroscopy. AJR. Am J Roentgenol. 1996;167(1):127–32.
10. Eckstein F, Charles HC, Buck RJ, Kraus VB, Remmers AE, Hudelmaier M, Wirth W, Evelhoch JL. Accuracy and precision of quantitative assessment of cartilage morphology by magnetic resonance imaging at 3.0 T. Arthritis Rheum. 2005;52(10):3132–6.
11. Siepmann DB, McGovern J, Brittain JH, Reeder SB. High-resolution 3D cartilage imaging with IDEAL–SPGR at 3 T. Am J Roentgenol. 2007;189(6):1510–5.
12. Bashir A, Gray ML, Hartke J, Burstein D. Nondestructive imaging of human cartilage glycosaminoglycan concentration by MRI. Magn Reson Med. 1999;41(5):857–65.
13. Liess C, Lüsse S, Karger N, Heller M, Glüer CC. Detection of changes in cartilage water content using MRI T2-mapping in vivo. Osteoarthr Cartil. 2002;10(12):907–13.
14. Mosher TJ, Dardzinski BJ, Smith MB. Human articular cartilage: influence of aging and early symptomatic degeneration on the spatial variation of T2—preliminary findings at 3 T. Radiology. 2000;214(1):259–66.
15. Link TM, Stahl R, Woertler K. Cartilage imaging: motivation, techniques, current and future significance. Eur Radiol. 2007;17:1135–46.
16. Stahl R, Luke A, Li X, Carballido-Gamio J, Ma CB, Majumdar S, Link TM. T1rho, T 2 and focal knee cartilage abnormalities in physically active and sedentary healthy subjects versus early OA patients—a 3.0-tesla MRI study. Eur Radiol. 2009;19(1):132–43.
17. Trattnig S, Millington SA, Szomolanyi P, Marlovits S. MR imaging of osteochondral grafts and autologous chondrocyte implantation. Eur Radiol. 2007;17(1):103–18.
18. Watanabe A, Obata T, Ikehira H, Ueda T, Moriya H, Wada Y. Degeneration of patellar cartilage in patients with recurrent patellar dislocation following conservative treatment: evaluation with delayed gadolinium-enhanced magnetic resonance imaging of cartilage. Osteoarthr Cartil. 2009;17(12):1546–53.
19. Trattnig S, Mlyńarik V, Breitenseher M, Huber M, Zembsch A, Rand T, Imhof H. MRI visualization of proteoglycan depletion in articular cartilage via intravenous administration of Gd-DTPA. Magn Reson Imaging. 1999;17(4):577–83.
20. Potter HG, Foo LF. Articular cartilage. In: Stoller DW, editor. Magnetic resonance imaging in orthopaedics and sports medicine. Philadelphia: Lippincott Williams & Wilkins; 2007.
21. Hunziker EB. Articular cartilage repair: basic science and clinical progress. A review of the current status and prospects. Osteoarthr Cartil. 2002;10(6):432–63.
22. Marlovits S, Singer P, Zeller P, Mandl I, Haller J, Trattnig S. Magnetic resonance observation of cartilage repair tissue (MOCART) for the evaluation of autologous chondrocyte transplantation: determination of interobserver variability and correlation to clinical outcome after 2 years. Eur J Radiol. 2006;57(1):16–23.
23. Schreiner MM, Raudner M, Marlovits S, Bohndorf K, Weber M, Zalaudek M, Röhrich S, Szomolanyi P, Filardo G, Windhager R, Trattnig S. The MOCART (magnetic resonance observation of cartilage repair tissue) 2.0 knee score and atlas. Cartilage. 2019:1947603519865308.
24. Mithoefer K, Williams RJ III, Warren RF, Potter HG, Spock CR, Jones EC, Wickiewicz TL, Marx RG. The microfracture technique for the treatment of articular cartilage lesions in the knee: a prospective cohort study. JBJS. 2005;87(9):1911–20.
25. Brown WE, Potter HG, Marx RG, Wickiewicz TL, Warren RF. Magnetic resonance imaging appearance of cartilage repair in the knee. Clin Orthop Relat Res. 2004;422:214–23.
26. Rubak JM. Reconstruction of articular cartilage defects with free periosteal grafts: an experimental study. Acta Orthop Scand. 1982;53(2):175–80.
27. Glenn RE Jr, McCarthy EC, Potter HG, et al. Comparison of fresh osteochondral autografts and allografts: a canine model. Am J Sports Med. 2006;34(7):1084–93. https://doi.org/10.1177/0363546505284846.
28. Verstraete KL, Almqvist F, Verdonk P, Vanderschueren GE, Huysse W, Verdonk R, Verbrugge G. Magnetic resonance imaging of cartilage and cartilage repair. Clin Radiol. 2004;59(8):674–89.
29. Alparslan L, Minas T, Winalski CS. Magnetic resonance imaging of autologous chondrocyte implantation. Semin Ultrasound CT MR. 2001;22(4):341–51.